Guided propagation along quadrupolar chains of plasmonic nanoparticles

Andrea Alù[1,2,*] and Nader Engheta[2]
[1]*Department of Electrical and Computer Engineering, University of Texas at Austin, Austin, Texas 78712, USA*
[2]*Department of Electrical and Systems Engineering, University of Pennsylvania, Philadelphia, Pennsylvania 19104, USA*
(Received 5 April 2009; published 12 June 2009)

The employment of periodic arrays of plasmonic nanoparticles has been proposed by several groups for enhanced transmission or absorption and for realizing optical nanowaveguides. Generally, due to their small transverse dimensions, such linear arrays have been operated near their dipolar resonance. However, it has been recently shown that nanoscale plasmonic particles may also support higher-order resonances, which provide some advantages in different applications. Here we derive a full-wave analytical closed-form dispersion equation for the guided and leaky modes supported by linear chains of nanoparticles near a quadrupolar resonance. We show that, despite the vanishing bandwidth of the individual quadrupolar resonance in each of the nanoparticles composing the chain, the overall bandwidth of quadrupolar chain guidance is relatively large due to strong coupling, even considering realistic losses and frequency dispersion of optical materials. Applications for low-damping optical nanotransmission lines and leaky-wave nanoantennas are suggested.

DOI: 10.1103/PhysRevB.79.235412 PACS number(s): 78.67.Bf, 42.70.Qs, 42.82.Et, 71.45.Gm

I. INTRODUCTION

Linear arrays of plasmonic nanoparticles have been recently proposed as novel optical waveguides.[1–12] Theoretical analyses have shown that it may indeed be possible to confine and guide an optical guided wave along a periodic array of nanoparticles near their resonance and, over a relatively large bandwidth, the guided beam would not significantly radiate. Experimental realizations of such arrays have also been presented by several groups, which to some extent have shown the possibility of achieving low-damping guided modes suitable for optical communications. In Ref. 10 we have presented a fully dynamic closed-form expression that may describe the modal propagation along these chains, even taking into account, in a full-wave model, radiation and absorption losses from the nanoparticles. In Ref. 11 we have extended it to three-dimensional (3D) arrays and in Ref. 12 we have also successfully modeled how the possible technological disorder may affect these guidance properties. All these works[1–12] have assumed that each nanoparticle composing the chain is near its dipolar (dominant) resonance, which is usually the case for small particles.

However, it is well known that plasmonic nanoparticles may support higher-order localized resonances at optical frequencies, even when their total size is much smaller than the wavelength of operation.[13–18] The second-order quadrupolar resonance has been suggested in theoretical[14–17] and experimental[18] works as a possible way to design optical nanoantennas with directive properties.[15–18]

When applied to guided modes, the quadrupolar resonance may have exciting potentials: heuristically, as depicted in Fig. 1(a), the classic dipolar chain behaves in many ways analogously to a regular single current wire at lower frequencies, indeed guiding the field along its axis, but also susceptible to radiation losses and field spreading in the background material. This is also consistent with the heuristic interpretation given in Ref. 10 in terms of optical nanocircuit elements composing the chain.[19,20] The two-wire transmission-line equivalent for this kind of propagation is depicted in Fig. 1(a) and it consists of cascades of inductors (the plasmonic nanoparticles) and capacitors (the gaps between them). By exciting quadrupolar polarization in each nanoparticle, however, the chain would operate as a nanotransmission line, as heuristically suggested in Ref. 21, consistent with Fig. 1(b). In this case, the radiation losses and field spreading should be much reduced, analogous to two parallel wires closely spaced, supporting oppositely directed currents at low frequency. The circuit equivalent may also be accordingly modified, as in Fig. 1(b). In their leaky mode operation, one would expect enhanced directivity from such modal regime, analogous to the metamaterial leaky-wave antennas.[22,23] In their guided mode operation, due to the field confinement and reduced radiation leakage, one would expect operation consistent with a regular transmission line at low frequencies.[22,23]

Here we model in closed form the full-wave dynamic problem of guided and complex modes supported by an infinite linear chain of quadrupolar particles, taking into account also losses and frequency dispersion in the materials involved. Following a solution analogous to the one considered in Ref. 10 for dipolar chains, but here applied to quadrupolar particles, it is possible to write the modal equation in closed form, even considering complex propagation constants and the entire coupling among the infinite nanoparticles. In this way, we can derive the fundamental limits and properties of the modes supported by such chains, and then compare them with the case of dipolar arrays. We show that the heuristic operation of Fig. 1 is present, and interesting modal properties are described for these linear chains of quadrupolar nanoparticles. Applications for optical waveguides and directive leaky-wave nanoantennas are envisioned.

II. FUNDAMENTAL PROPERTIES OF GUIDED MODES ALONG QUADRUPOLAR CHAINS

A. Quadrupolar fields and interaction

A given electric field distribution $\mathbf{E}_0(\mathbf{r})$ impinging on a nanoparticle located at the point $\mathbf{r}=\mathbf{r_0}$ excites different scat-

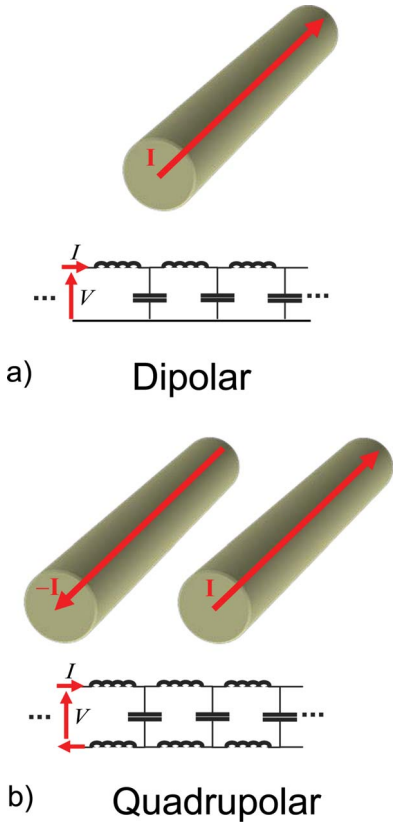

FIG. 1. (Color online) Analogy between the (a) dipolar or (b) quadrupolar operation of a linear chain of nanoparticles, its low-frequency interpretation in terms of currents traveling along conducting wires, and corresponding circuit models.

tering multipolar orders. In the case of small nonresonant particles, the electric-dipole moment $\mathbf{p}$ is dominant, with an amplitude proportional to the local electric field $\mathbf{p}=\alpha_e\mathbf{E}_0(\mathbf{r})$, with α_e being the electric polarizability of the particle. In general, however, higher-order multipole moments may be excited as well. Expanding the field distribution in Taylor series around the point $\mathbf{r_0}$, one gets

$$\mathbf{E}_0(\mathbf{r}) = \mathbf{E}_0(\mathbf{r}_0) + \frac{1}{2}\nabla\,\mathbf{E}_0(\mathbf{r}_0)\cdot(\mathbf{r}-\mathbf{r}_0) + \cdots, \tag{1}$$

each of the terms in this series contributes to the excitation of a particular multipolar spherical harmonic.[24] Indeed, if one also expands in Taylor series the equivalent induced polarization current on the particle, one may write the scattered field as a superposition of the radiation from different multipoles,[25]

$$\mathbf{E}_{scat}(\mathbf{r}) = \mathbf{p}\cdot + \frac{1}{2}\underline{\mathbf{Q}}\cdot\nabla(\mathbf{r}-\mathbf{r}_0) + \frac{1}{2}\mathbf{m}\cdot\nabla\times(\mathbf{r}-\mathbf{r}_0)\cdots. \tag{2}$$

Here we focus on the electric-quadrupole moment tensor $\underline{\mathbf{Q}}$, which we assume to be the dominant response from each nanoparticle. Being a traceless tensor, $\underline{\mathbf{Q}}$ interacts only with the symmetric part of the gradient of the electric field.[25,26] We may therefore define the electric *quadrupolarizability* of a nanoparticle α_q through the tensorial expression,[27]

$$\underline{\mathbf{Q}} = \alpha_q\frac{\nabla\mathbf{E}_0 + \mathbf{E}_0\nabla}{2}. \tag{3}$$

As an aside, the antisymmetric part of the gradient of the field, which is proportional to its curl and therefore to the magnetic field [since $\frac{\nabla\mathbf{E}_0-\mathbf{E}_0\nabla}{2}=\frac{1}{2}(\nabla\times\mathbf{E}_0)\times\underline{\mathbf{I}}=\frac{i\omega\mu_0}{2}\mathbf{H}_0\times\underline{\mathbf{I}}$ (Ref. 28)], is responsible for the excitation of the magnetic-dipole moment $\mathbf{m}$. (Since the magnetic-dipole moment is an axial vector, it interacts only with the asymmetric part of the gradient of the electric field, which in fact is proportional to its curl.) Using the previous tensorial notation, we may write the proportionality relation $\underline{\mathbf{m}}=\mathbf{m}\times\underline{\mathbf{I}}=\frac{2\alpha_m}{i\omega\mu_0}\frac{\nabla\mathbf{E}_0-\mathbf{E}_0\nabla}{2}$, which corresponds to the usual $\mathbf{m}=\alpha_m\mathbf{H}_0$ with α_m being the magnetic polarizability of the particle. This clearly distinguishes the magnetic and the quadrupolar features of the nanoparticles that we are considering here. In the previous expressions and in the following, ω is the radian frequency (under the $e^{-i\omega t}$ notation) and μ_0 is the background permeability. Similarly, higher-order multipoles may be related to the higher-order spatial derivatives of the electric field through similar proportionality coefficients. In general, these proportionality factors, and in particular α_q, may be regarded as dyadics of proper rank, taking into account the possible particle anisotropy. In the following, however, for sake of simplicity, we consider α_q to be a scalar, implying that the nanoparticle response is isotropic, or focusing more on a specific polarization of the field and of its derivatives.

Usually an electrically small nanoparticle has a dominant electric polarizability, as in the cases analyzed in Ref. 1–12 and its response may be well modeled by the term α_e. Recently, however, it has been shown the possibility of inducing a higher-order polaritonic resonance in a small nanoparticle partially filled with metamaterials or plasmonic materials with negative constitutive parameters.[14–18] This implies that under specific conditions the quadrupolar response of a subwavelength plasmonic nanoparticle may become dominant. Near this resonance, which usually has a limited bandwidth and very high Q resonance factor, the particle may be successfully described by α_q, dominant over any other polarizability coefficient. In this case, the nanoparticle would mainly interact with the symmetric gradient of the electric field, rather than the field itself, consistent with the previous discussion and the considerations in Ref. 16 in which such quadrupolar particles have been operated as directive nanoantennas.

The nanoparticle radiation and scattering may be described by the vector potential $\mathbf{A}$ as[25]

$$\mathbf{A}(\mathbf{r}) = \frac{i\omega\mu_0}{8\pi}\underline{\mathbf{Q}}\cdot\nabla\frac{e^{ik_0 r}}{r}, \tag{4}$$

with magnetic and electric fields obtained as $\mathbf{H}=\mu_0^{-1}\nabla\times\mathbf{A}$, and $\mathbf{E}=(-i\omega\varepsilon_0)^{-1}\nabla\times\mathbf{H}$ with ε_0 being the background electric permittivity.

The total averaged radiated power by a quadrupole of amplitude $\underline{\mathbf{Q}}$ is then obtained by integrating the quantity $\mathrm{Re}[\mathbf{E}\times\mathbf{H}^*]/2$ over any mathematical surface enclosing the nanoparticle, yielding

$$P_{rad} = \frac{\|\underline{\mathbf{Q}}\|^2 \omega k_0^5}{40\pi\varepsilon_0}, \tag{5}$$

where $\|\underline{\mathbf{Q}}\|^2$ is the sum of the squared absolute values of the dyadic elements and $k_0 = \omega\sqrt{\varepsilon_0\mu_0}$ is the background wave number.

It should be underlined that the assumption that the particle is near its quadrupolar resonance ensures that even an observer placed very close to the particle surface would measure a field distribution dominated by this quadrupolar term. This implies that in considering the mutual interaction between particles (near their quadrupolar resonance) arranged in a chain, it is sufficient to consider their α_q, even when their center-to-center distance is rather small.

B. Properties of α_q

It is worth noting now that the second-order transverse magnetic (TM) spherical wave in the Mie scattering expansion[29] coincides with the quadrupolar radiation described by Eq. (4). In comparing this expression with that of the scattering from a particle illuminated by a plane wave with $\mathbf{E}_{pw} = \hat{\mathbf{x}} E_0 e^{ik_0 z}$, one may write the following relation between the Mie scattering coefficient c_2^{TM} as defined in Ref. 14 and the induced quadrupole moment $\underline{\mathbf{Q}} = Q(\hat{\mathbf{x}}\hat{\mathbf{x}} + \hat{\mathbf{z}}\hat{\mathbf{z}})$,

$$Q = \frac{20\pi\varepsilon_0 E_0 c_2^{TM}}{k_0^4}. \tag{6}$$

Moreover, since $\frac{\nabla \mathbf{E}_{pw} + \mathbf{E}_{pw}\nabla}{2} = \frac{ik_0 E_0}{2}(\hat{\mathbf{x}}\hat{\mathbf{x}} + \hat{\mathbf{z}}\hat{\mathbf{z}})$, we get the interesting relation:

$$\alpha_q = -\frac{40\pi i \varepsilon_0 c_2^{TM}}{k_0^5}, \tag{7}$$

which directly relates the quadrupolarizability of a particle to its second-order Mie TM scattering coefficient c_2^{TM}. This is interestingly analogous to the formula $\alpha_e = -6\pi i \varepsilon_0 c_1^{TM} k_0^{-3}$ derived in Ref. 10 for the electric polarizability and it may be extended and generalized to all other polarizability coefficients.

In Ref. 14 we have discussed how the Mie scattering coefficient may be written as

$$c_2^{TM} = -\frac{U_2^{TM}}{U_2^{TM} + iV_2^{TM}}, \tag{8}$$

where U_2^{TM} and V_2^{TM} are real functions when the particle is lossless and the background is transparent (i.e., $k_0 \in \mathbb{R}$). As an example, the expressions of U_2^{TM} and V_2^{TM} for a two-layered core-shell sphere are reported in Ref. 14. The quardupolar resonance arises in this case when $V_2^{TM} = 0$, implying that c_2^{TM} reaches its maximum value, i.e., $c_2^{TM} = -1$ and $\alpha_q = \frac{40\pi i \varepsilon_0}{k_0^5}$, which becomes a purely imaginary quantity (as a symptom of the resonant phenomenon, in fact, the induced quadrupole moment is 90° out of phase with the impinging excitation, in order to extract maximum energy). It is interesting to see that expression (8), when lossless particles and transparent background is assumed, implies that $\mathrm{Re}[(c_2^{TM})^{-1}] = -1$, and therefore

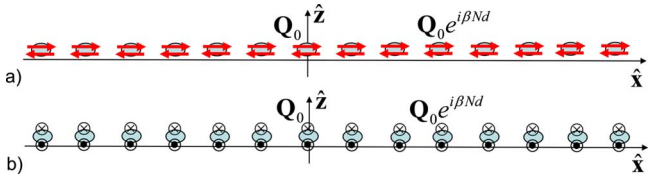

FIG. 2. (Color online) Geometry of the problem: an array of quadrupolar nanoparticles supporting a (a) longitudinal or (b) transverse mode.

$$\mathrm{Im}[\alpha_q^{-1}] = -\frac{k_0^5}{40\pi\varepsilon_0}, \tag{9}$$

a general condition totally independent of the nature and geometry of the particle, and analogous to the relation for the electric polarizability of a lossless particle $\mathrm{Im}[\alpha_e^{-1}] = -\frac{k_0^3}{6\pi\varepsilon_0}$.[2,9,10]

Equation (9) descends directly from power conservation relations, as it may be confirmed by equating the power that the quadrupole extracts from the impinging field $\mathbf{E}_{pw}$, which is

$$P_{ext} = \frac{1}{2}\mathrm{Re}\left[\frac{i\omega Q^*}{2}\left(\frac{\partial E_z}{\partial x} + \frac{\partial E_x}{\partial z}\right)\right] = \frac{1}{2}\mathrm{Re}\left[\frac{i\omega}{4}\alpha_q^*\left|\frac{\partial E_z}{\partial x} + \frac{\partial E_x}{\partial z}\right|^2\right] = \frac{\omega}{8}\left|\frac{\partial E_z}{\partial x} + \frac{\partial E_x}{\partial z}\right|^2 \mathrm{Im}[\alpha_q], \tag{10}$$

with the power radiated by the same quadrupole, given by Eq. (5),

$$P_{rad} = \frac{|Q|^2 \omega k_0^5}{80\pi\varepsilon_0} = \frac{\omega k_0^5}{320\pi\varepsilon_0}|\alpha_q|^2\left|\frac{\partial E_z}{\partial x} + \frac{\partial E_x}{\partial z}\right|^2. \tag{11}$$

Imposing $P_{ext} = P_{rad}$ one reobtains Eq. (9), completely independent of any assumption on the nature of the nanoparticle. Similar to the dipolar case, the quadrupolar resonance of an isolated particle in the lossless limit may therefore be simply indicated by the condition $\mathrm{Re}[\alpha_q^{-1}] = 0$ since the imaginary part of α_q^{-1} is governed by Eq. (9) and it is independent of the particle specific geometry. When small Ohmic losses are present, they add an additional negative contribution to the right-hand side of Eq. (9), taking into account the absorption losses, while they do not sensibly affect this resonance condition.

C. Dispersion relations

Consider now the case of an infinite array of such quadrupolarizable particles, as depicted in Fig. 2, arranged along the x axis at the location $x = Nd$ with N being any integer. Let $\underline{\mathbf{Q}}_N$ be the quadrupole moment excited on each of these particles. Suppose now that the particle at $x = 0$ is excited by a given electric field distribution, inducing the quadrupole moment $\underline{\mathbf{Q}}_0$. Without loss of generality we may split the problem into the two orthogonal cases: longitudinal polarization, for which $\underline{\mathbf{Q}}_0 = Q(\hat{\mathbf{x}}\hat{\mathbf{x}} + \hat{\mathbf{z}}\hat{\mathbf{z}})$, as in Fig. 2(a), and transverse polarization, for which $\underline{\mathbf{Q}}_0 = Q(\hat{\mathbf{y}}\hat{\mathbf{y}} + \hat{\mathbf{z}}\hat{\mathbf{z}})$, as in Fig. 2(b).

The field radiated by $\underline{\mathbf{Q}}_0$ in one of these two polarizations may be obtained from Eq. (4) and it would induce at other locations $x=Nd$ other quadrupoles with the same polarization, i.e., $\underline{\mathbf{Q}}_N \| \underline{\mathbf{Q}}_0 \forall N$. We look for the conditions under which a propagating mode in the form $\underline{\mathbf{Q}}_N = \underline{\mathbf{Q}}_0 e^{i\beta Nd}$ may be self-sustained by such a chain with a small, or even a null, damping factor (i.e., $\mathrm{Im}[\beta] \simeq 0$), as depicted in Fig. 2.

In the fully dynamic case, the dispersion relations for these modes may be found by imposing that the symmetric part of the gradient of the electric field induced at the location $x=0$ by the infinite chain of quadrupoles $\underline{\mathbf{Q}}_N = \underline{\mathbf{Q}}_0 e^{i\beta Nd}$ (with $N \neq 0$) equals the one necessary to sustain $\underline{\mathbf{Q}}_0$, analogous to the analyses for the dipolar chain presented in Refs. 2 and 10. In our notation they may be written in the following normalized form for the two polarizations:

$$L: 5\sum_{N=1}^{\infty} [N^{-5}\bar{d}^{-5}\cos(N\bar{\beta}\bar{d})e^{iN\bar{d}}(48 - 48iN\bar{d} - 21N^2\bar{d}^2 + 5iN^3\bar{d}^3 + N^4\bar{d}^4)] = \bar{\alpha}_q^{-1},$$

$$T: -10\sum_{N=1}^{\infty} [N^{-5}\bar{d}^{-5}\cos(N\bar{\beta}\bar{d})e^{iN\bar{d}}(6 - 6iN\bar{d} - 3N^2\bar{d}^2 + iN^3\bar{d}^3)] = \bar{\alpha}_q^{-1}, \tag{12}$$

where $\bar{d}=k_0 d$, $\bar{\beta}=\beta/k_0$, $\bar{\alpha}_q = k_0^5 \alpha_q/(40\pi\varepsilon_0)$. In this way all the quantities involved in Eq. (12) are dimensionless and the equations are frequency invariant. The dispersion equations are even with β, as expected from the reciprocity of the chain, and they are periodic with principal Floquet period $-\pi/\bar{d} < \bar{\beta} < \pi/\bar{d}$.

For the two polarizations, Eq. (12) is a complex equation and the summation on the left-hand side diverges for complex solutions of β, as already noted in the dipolar case.[10] The dispersion equations, however, may be analytically continued in the complex plane by using polylogarithm functions $Li_n(.)$,[30] as we did for the dipolar solution, obtaining here,

$$L: \frac{5}{2}\bar{d}^{-5}[48f_5 - 48i\bar{d}f_4 - 21\bar{d}^2 f_3 + 5i\bar{d}^3 f_2 + \bar{d}^4 f_1] = \bar{\alpha}_q^{-1},$$

$$T: -5\bar{d}^{-5}[6f_5 - 6i\bar{d}f_4 - 3\bar{d}^2 f_3 + i\bar{d}^3 f_2] = \bar{\alpha}_q^{-1}, \tag{13}$$

with $f_N = Li_N(e^{i(\bar{\beta}+1)\bar{d}}) + Li_N(e^{-i(\bar{\beta}-1)\bar{d}})$.

Formulation (13) provides a completely general closed-form dispersion equation for all the modes supported by a quadrupolar chain, valid for any complex value of the parameters coming into play and fully capable of taking into account the presence of material absorption and radiation losses. We stress here that Eq. (13) takes into account of the full dynamic coupling among the infinite number of nanoparticles composing the arrays of Fig. 2, with the only approximation of describing them as pure quadrupoles, i.e., neglecting the other multipoles contributing to their radiation and scattering. This assumption is valid as long as the nanoparticles are near their quadrupolar resonance, which, as we show in the following, is necessary for the existence of the guided modes analyzed here. This analytical expression is the main result of this paper, and in the following we discuss and analyze in details the modal properties of these chains by utilizing these equations. It is noticed that propagation from short arrays of nanoparticles with quadrupolar contributions has been theoretically explored in Ref. 17. Our results here, however, represent an extensive and rigorous analysis of the overall eigenmodal propagation properties of the long chains and their comparison with guidance along dipolar arrays.

D. Power conservation and consistency of the dispersion equations

In the case of a transparent background, i.e., for $k_0 \in \mathbb{R}$, real solutions of $\bar{\beta}$ for Eqs. (12) and (13) would correspond to propagating modes along the chain that do not radiate energy and do not decay. By extracting the imaginary part of Eq. (13) under the hypothesis of real $\bar{\beta}$, and noticing that[30,31]

$$\begin{cases} Li_1(e^{i\theta}) = Cl_1(\theta) + i\dfrac{(\pi-\theta)}{2} \\ Li_2(e^{i\theta}) = \dfrac{\pi^2}{6} - \dfrac{\theta(2\pi-\theta)}{4} + iCl_2(\theta) \\ Li_3(e^{i\theta}) = Cl_3(\theta) + i\dfrac{\theta(\pi-\theta)(2\pi-\theta)}{12} \\ Li_4(e^{i\theta}) = \dfrac{8\pi^4 - 60\pi^2\theta^2 + 60\pi\theta^3 - 15\theta^4}{720} + iCl_4(\theta) \\ Li_5(e^{i\theta}) = Cl_5(\theta) + i\dfrac{\theta(\pi-\theta)(2\pi-\theta)(4\pi^2 + 6\pi\theta - 3\theta^2)}{720} \end{cases} \qquad 0 \leq \theta \leq 2\pi, \tag{14}$$

where $Cl_N(\theta)$ are Clausen's functions,[30] which are real for real argument, we may get the following interesting closed-form relations, analogous to those obtained for the dipolar chain problem,

$$\begin{cases} L:\mathrm{Im}[\bar{\alpha}_q^{-1}] = -1 \\ T:\mathrm{Im}[\bar{\alpha}_q^{-1}] = -1 \end{cases} \quad \text{for } 1 < |\bar{\beta}| < \pi/\bar{d},$$

$$\begin{cases} L:\mathrm{Im}[\bar{\alpha}_q^{-1}] = -1 + 5\pi(1 - 3\bar{\beta}^2 + 4\bar{\beta}^4)/(4\bar{d}) \\ T:\mathrm{Im}[\bar{\alpha}_q^{-1}] = -1 + 5\pi(1 - \bar{\beta}^4)/(4\bar{d}) \end{cases} \quad \text{for } 0 < |\bar{\beta}| < 1. \tag{15}$$

Equation (15) represents an important result: it ensures that power conservation is satisfied and that ideal eigenmode guidance is possible along lossless quadrupolar chains. When $|\bar{\beta}| > 1$ the interference among the quadrupolar fields of each particle is destructive at any "visible" angle, leading to the propagation of a nonradiating, confined and guided wave along the chain, whose field distribution decays in the radial direction as $K_2(\sqrt{\beta^2 - k_0^2}\sqrt{y^2+z^2})$ and $K_3(\sqrt{\beta^2 - k_0^2}\sqrt{y^2+z^2})$ for the longitudinal and transverse polarizations, respectively, where $K_n(.)$ is the modified cylindrical Bessel function (these are one order higher than the corresponding Bessel functions in the dipolar chain,[10] ensuring higher field confinement along quadrupolar chains of nanoparticles. This is consistent with the heuristic interpretation of Fig. 1). In this case, as expected, the real-valued solutions of β for Eq. (13) are admitted if the particles are lossless since the condition $\mathrm{Im}[\bar{\alpha}_q^{-1}] = -1$ is consistent with Eq. (9). This situation, which is of interest in the present paper, is achievable only for $\bar{d} < \pi$, similar to the dipolar chain. When $|\bar{\beta}| < 1$, a positive term is added to the right-hand side of Eq. (15), taking into account of the power loss due to leaky-wave radiation from the chain. It is interesting that this additional term is smaller, for the same value of $\bar{\beta}$, compared to the one evaluated in Ref. 10 for dipolar chains, implying reduced radiation losses and more directivity for the supported leaky modes in these quadrupolar chains, consistent again with the earlier discussion for Fig. 1.

Remaining in the lossless limit and seeking for no-damped guided modes under the necessary conditions $\bar{d} < \pi$ and $1 < |\bar{\beta}| < \pi/\bar{d}$, the real part of Eq. (13) determines the guidance properties of these modes as a function of $\mathrm{Re}[\bar{\alpha}_q^{-1}]$, which is directly related to the nanoparticle geometry. Using Eq. (14), in this case we can write

$$L:\mathrm{Re}[\bar{\alpha}_q^{-1}] = \frac{5}{2}\bar{d}^{-5}[48g_5 + 48\bar{d}g_4 - 21\bar{d}^2 g_3 - 5\bar{d}^3 g_2 + \bar{d}^4 g_1],$$

$$T:\mathrm{Re}[\bar{\alpha}_q^{-1}] = -5\bar{d}^{-5}[6g_5 + 6\bar{d}g_4 - 3\bar{d}^2 g_3 - \bar{d}^3 g_2], \tag{16}$$

with $g_N = Cl_N[(\bar{\beta}+1)\bar{d}] + Cl_N[(-\bar{\beta}+1)\bar{d}]$.

The dispersion properties for the two polarizations in Eq. (16) are quite distinct, and richer than those in the dipolar case. We analyze them in details in the following.

E. Longitudinal polarization

In the longitudinal polarization, corresponding to Fig. 2(a), the dispersion curve of $\mathrm{Re}[\bar{\alpha}_q^{-1}]$ versus $\bar{\beta}$ is monotonic for any value of $\bar{d}$, similar to the longitudinal modes in a regular dipolar chain. However, quite distinctly here, the quadrupolar chain does not support a smooth transition between guided modes and leaky modes in this polarization. The dispersion diagram for the guidance region is shown in Fig. 3, reporting the values of normalized quadrupolarizability that support guidance for a given $\bar{d}$. Guidance is supported in the region above the red dashed line: any value of quadrupolarizability larger than those lying on the red dashed line ($\bar{\beta} = \pi/\bar{d}$) would in principle support a guided longitudinal mode, with no upper limits. However, increasing $\mathrm{Re}[\bar{\alpha}_q^{-1}]$ reduces $\bar{\beta}$ quite fast, as the different curves for equal values of guided wave number $\bar{\beta}$ show. The black solid line, for instance, delimits the modes for which $\bar{\beta} = 1.001$, whose field confinement is already compromised. In practice, the guidance region is limited to the range of values around the quadrupolar resonance, and this region widens up sensibly for closely packed chains, similar to the dipolar case (notice that the vertical axis here is normalized to $\bar{d}^5$). In particular, for $\bar{d} \to 0$ the guidance region may be written in exact closed form as

$$L: -225\xi(5) \le \bar{d}^5\,\mathrm{Re}[\bar{\alpha}_q^{-1}] \le 240\xi(5), \tag{17}$$

with $\xi(.)$ being the Riemann zeta function. This is an interesting result for the required values of quadrupolarizabilities in order to support a guided mode.

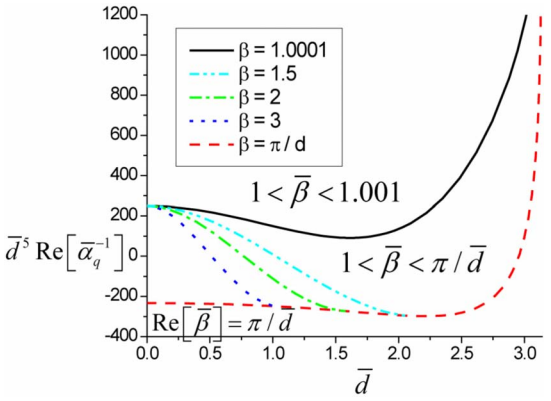

FIG. 3. (Color online) Region of guidance for longitudinally polarized modes [Fig. 2(a)]. Longitudinal modes are supported for any value of polarizability above the red dashed line.

To provide an example of the modal dispersion for this longitudinal polarization, Fig. 4 reports two typical dispersion curves, for narrow spacing [$\bar{d}=0.1$, Fig. 4(a)] and large spacing [$\bar{d}=0.9\pi$, Fig. 4(b)], respectively. The exact dispersion lines are compared with the nearest-neighbor approximation (NNA), i.e., the approximate solution obtained considering only the quasistatic quadrupolar interaction between nearest neighboring particles, obtained from Eq. (12) by truncating the summation to the first term and neglecting the imaginary part of the solution (which is vanishing for small $\bar{d}$). It can be seen how NNA is valid for small $\bar{d}$, but it is not sufficiently precise when the nanoparticles are further apart, for which the dynamic full-wave coupling among the infinite quadrupoles is required. In both cases, as also confirmed from Fig. 3, the slope $\frac{\partial\bar{\beta}}{\partial \mathrm{Re}[\bar{\alpha}_q^{-1}]}<0$, which corresponds to forward propagation, analogous to what we have shown analytically in Ref. 10. Longitudinal modes are indeed forward (parallel group and phase velocities) for any point in the guidance region of Fig. 3. It is worth noting the very different horizontal scale of admissible values of $\mathrm{Re}[\bar{\alpha}_q^{-1}]$ in the two plots, consistent with Eq. (17).

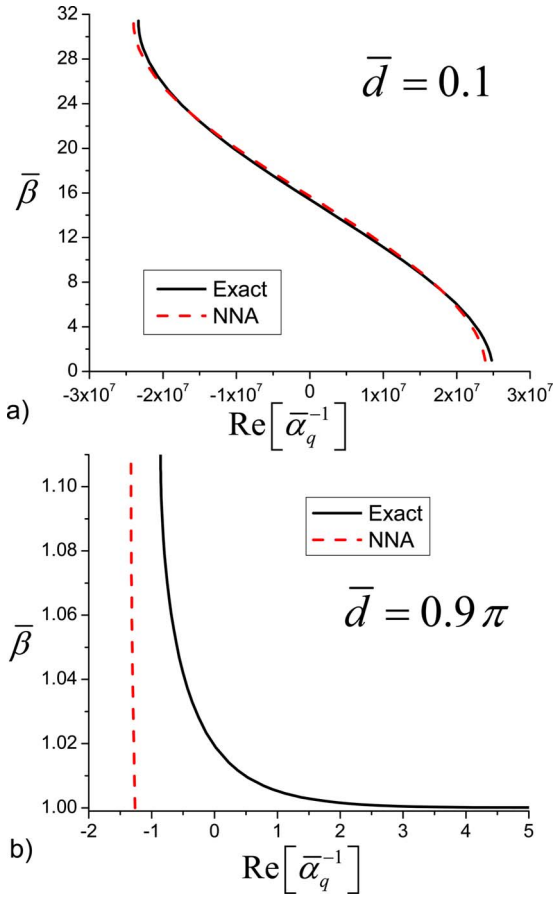

FIG. 4. (Color online) Dispersion plots for the guided mode for the longitudinal polarization in terms of the particle's quadrupolarizability, for two different values of spacing.

F. Transverse polarization

The analysis for the transverse polarization, corresponding to Fig. 2(b), is more challenging. Over most of the guidance region $1<|\bar{\beta}|<\pi/\bar{d}$ its dispersion is monotonic, implying that the allowed values of $\mathrm{Re}[\bar{\alpha}_q^{-1}]$ are included between its extreme values calculated for $\bar{\beta}=1$ and $\bar{\beta}=\pi/\bar{d}$. This range may be written in closed form, by applying Eq. (14) and the identities $Li_2(1)=\pi^2/6$, $Li_4(1)=\pi^4/90$, and $Li_{2N+1}(1)=\xi(2N+1)$, as

$$T{:}\bar{d}^5\ \mathrm{Re}[\bar{\alpha}_q^{-1}] \in \begin{bmatrix} 10[6Cl_5(\bar{d}+\pi)-6\bar{d}Cl_4(\bar{d}+\pi)+3\bar{d}^2Cl_3(\bar{d}+\pi)+\bar{d}^3Cl_2(\bar{d}+\pi)], \\ -5[\xi(5)+\xi(3)+6Cl_5(2\bar{d})+6\bar{d}Cl_4(2\bar{d})-3\bar{d}^2Cl_3(2\bar{d})-\bar{d}^3Cl_2(2\bar{d})] \end{bmatrix} \tag{18}$$

This represents the closed-form expression for the range of normalized quadrupolarizabilities required for the particles to support guided transverse modes, as a function of their normalized distance. Figure 5 depicts this region: the black solid line corresponds to $\bar{\beta}=1$, which is the border between guided and leaky-wave regime, whereas the red dashed line is the locus of $\bar{\beta}=\pi/\bar{d}$, beyond which the complex evanescent Floquet modes with $\mathrm{Re}[\bar{\beta}]=\pi/\bar{d}$ are supported. In the region between the two lines transverse guided modes with no damping (in this limit of no losses) are admitted. However, it is evident that the two lines interestingly cross each other at $\bar{d}=2.06$, implying that a drastic change in the modal dispersion arises around this specific normalized distance. Curves for different values of $\bar{\beta}$ are also shown in the plot. The region between the blue dash-dotted line and the red dashed line, for instance, is that for which $\bar{\beta}>3$ (highly confined slow-wave modes). For small distances ($\bar{d}<2.06$) it is evident that an increase in the inverse quadrupolarizability increases the value of $\bar{\beta}$ and therefore the modal confinement around the chain. This is the opposite to the case of the longitudinal modes, a symptom of backward-wave propagation, similar to confined transverse modes supported by dipole chains.[10] However, for $\bar{d}>2.06$ the situation is reversed: the slope $\frac{\partial\bar{\beta}}{\partial \mathrm{Re}[\bar{\alpha}_q^{-1}]}$ flips its sign and forward modes are supported. In a narrow region around $\bar{d}=2.06$ the dispersion of $\bar{\beta}$ is nonmonotonic and two modes are supported for the same value of $\mathrm{Re}[\bar{\alpha}_q^{-1}]$, one forward and one backward, similar to transverse modes in dipolar chains.[10] In this regime, which is however limited to a narrow range of normalized distances $\bar{d}$

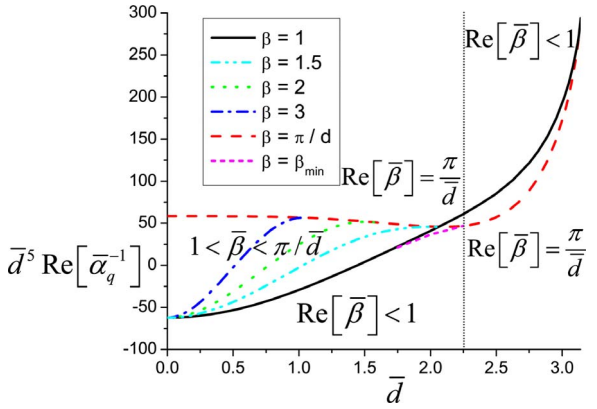

FIG. 5. (Color online) Region of guidance for transversely polarized modes [Fig. 2(b)].

around $\bar{d}=2.06$, the violet short-dashed line indicates the minimum value of $\mathrm{Re}[\bar{\alpha}_q^{-1}]$ that would support guided mode, with wave number $1<\bar{\beta}_{\min}<\pi/\bar{d}$.

For smaller $\bar{d}$, which is clearly the region of more interest, the guidance range for both longitudinal and transverse modes widens up (also here a factor of $\bar{d}^5$ is normalizing the vertical axis), being centered around the resonance condition for the isolated particle $\mathrm{Re}[\bar{\alpha}_q^{-1}]=0$. This implies that even if the bandwidth of quadrupolar resonance is usually very small for plasmonic nanoparticles,[15,16] the coupling among closely spaced elements may significantly increase the bandwidth for the guided mode of operation in both polarizations.[10,11] When the distance among particles is increased, the admissible quadrupolarizability range narrows down since the particles are required to be closer to their collective resonance to support a guided mode. When $\bar{d}\rightarrow\pi$ in this transverse propagation, the range of required polarizabilities tends to a single specific value for which $\bar{\beta}\rightarrow 1^+$, which may be written in closed form as $\mathrm{Re}[\bar{\alpha}_q^{-1}]=30\pi^{-3}[\xi(3)-2\pi^{-2}\xi(5)]\simeq 0.96$. This is the only possible quadrupolarizability value that would support a collective resonance when the spacing is $d=\lambda_0/2$ (λ_0 is the free space wavelength). Notice how this value is actually quite far from the individual quadrupolar resonance of the individual particles $\mathrm{Re}[\bar{\alpha}_q^{-1}]=0$.

Figure 6 reports the dispersion diagrams of real $\bar{\beta}$ versus $\mathrm{Re}[\bar{\alpha}_q^{-1}]$ for the transverse modes guided by an infinite array of lossless particles in three significant cases: narrow spacing [$\bar{d}=0.1$, Fig. 6(a)], anomalous guidance region [$\bar{d}=2.06$, Fig. 6(b)] and large spacing [$\bar{d}=0.9\pi$, Fig. 6(c)]. Consistent with the previous discussion, in the case of narrow spacing [Fig. 6(a)] $\bar{\beta}$ may yield large values, limited by $\pi/\bar{d}$, and the NNA predicts the dispersion reasonably well, since the coupling between neighboring particles dominates. In this regime, the slope $\frac{\partial\bar{\beta}}{\partial\,\mathrm{Re}[\bar{\alpha}_q^{-1}]}$ is positive, implying backward modes as discussed above. In the anomalous dispersion region [Fig. 6(b)], the dispersion curve presents a minimum, characterized by zero group velocity, for which $\bar{\beta}=\bar{\beta}_{\min}$ from Fig. 3, and the simultaneous presence of two modes for the same value of quadrupolarizability. In this narrow region, the two-mode

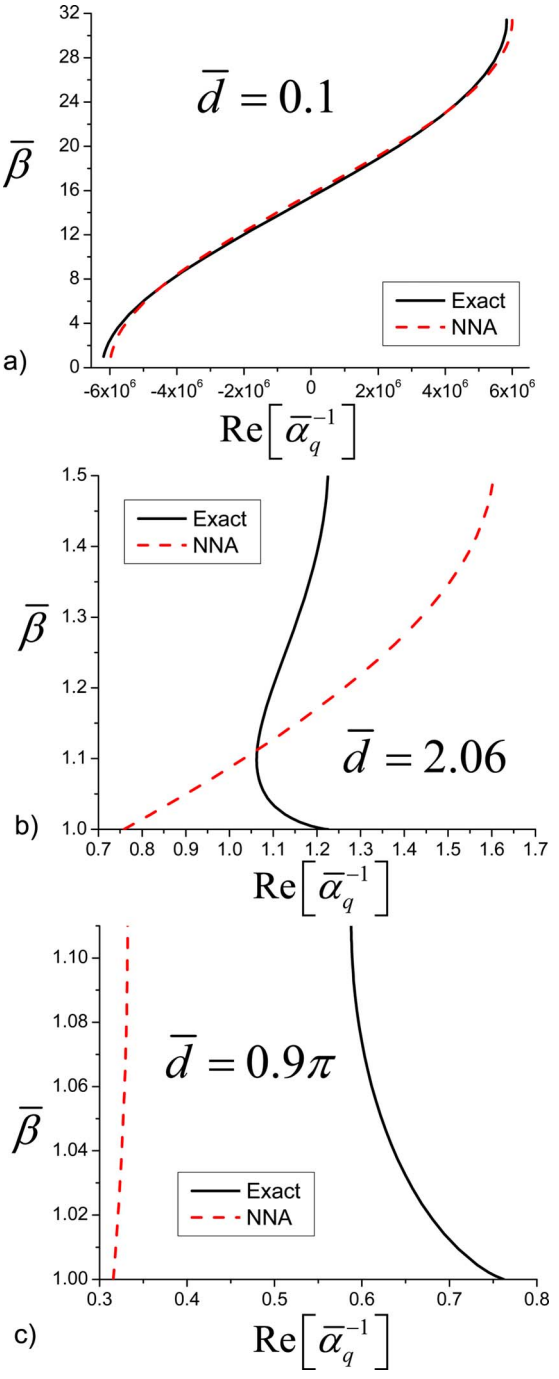

FIG. 6. (Color online) Dispersion plots for guided mode in transverse polarization in terms of the quadrupolarizability, for three different spacing values [(a) narrow spacing, (b) anomalous dispersion region, and (c) large spacing].

guidance is analogous to the transverse propagation in dipolar chains.[10]

For larger spacing [Fig. 6(c)], the guidance is limited to a narrow range of polarizabilities, consistent with Fig. 5, and the mode is poorly confined along the chain, since $\bar{\beta}\simeq 1$. The slope of the curve is opposite for the small and large spacing, consistent with the previous discussion on the transition between the backward and forward modes arising in the anomalous dispersion region for transversely polarized qua-

drupolar chains. The NNA cannot predict these complex dispersion features, as the curves in Figs. 4(b) and 4(c) show.

G. Presence of material and radiation losses along the chain

As pointed out above, Eq. (13) is also valid for complex values of $\bar{\beta}$. This implies that the leaky-wave regime $\mathrm{Re}[\bar{\beta}]<1$ and/or the presence of material absorption and radiation losses may be fully taken into account within this analysis. In particular, we consider here the presence of realistic Ohmic losses in the particle polarizability. It is interesting to underline that, following our results in Ref. 12, random disorder along the chain would produce radiation losses that may also be modeled as equivalent additional loss uniformly distributed across the particles. Under this assumption, damped propagation and a nonzero imaginary part of $\bar{\beta}$ are expected. The imaginary part of the inverse quadrupolarizability may be written as

$$\mathrm{Im}[\bar{\alpha}_q^{-1}] = -1 - \bar{\alpha}_{loss}^{-1}, \tag{19}$$

where $\bar{\alpha}_{loss}^{-1}>0$ for passive particles.

Following a line of reasoning analogous to the one reported in Ref. 10 for dipolar chains, we can show that for moderate losses the imaginary part of $\bar{\beta}$ may be written as

$$\bar{\beta}_i = \mathrm{Im}[\bar{\beta}] = -\bar{\alpha}_{loss}\frac{\partial\,\mathrm{Re}[\bar{\beta}_r]}{\partial\,\mathrm{Re}[\bar{\alpha}_q^{-1}]}, \tag{20}$$

i.e., it is proportional to the amount of losses in the nanoparticles and to the slope of the dispersion curve. This implies that low-damped propagation of guided mode may be achieved for closely spaced chains and in the middle of the guidance region of the dispersion plots, far from the edges of the guidance band for which the group velocity and $\frac{\partial\,\mathrm{Re}[\bar{\alpha}_q^{-1}]}{\partial\,\mathrm{Re}[\bar{\beta}_r]}$ get close to zero. This is consistent with analogous properties of dipolar chains.[10]

It is clear that the condition for minimum damping for a given quadrupolar chain is given by $\partial^2\,\mathrm{Re}[\bar{\alpha}_q^{-1}]/\partial\,\mathrm{Re}[\bar{\beta}]^2=0$, which may be written in closed form from Eq. (16) (not reported here for sake of brevity). For a given spacing $\bar{d}$ the optimum value of $\bar{\beta}$ is plotted in Fig. 7(a), after having been normalized to $\bar{d}^{-1}$ in both polarizations. As clearly evident from the previous expressions, when the spacing gets small, i.e., for $\bar{d}\to 0$, the optimum beta tends to 1.46 in both polarizations, a larger value than the case of dipolar chains. When the spacing is increased, the two polarizations behave differently, as seen from the plots. If in the longitudinal polarization this value of $\bar{\beta}$ quickly converges to a value near unity and then the minimum loss (which is zero) beyond this value is simply obtained for $\bar{\beta}=1$ when the mode is not confined any more, the transverse polarization in this sense offers a wider range of spacing values where a laterally confined mode allows to achieve the minimum loss condition. Such ranges are wider and thus offer comparatively better performance than the dipolar chain configuration, once again confirming the heuristic prediction of Fig. 1 that quadrupolar chains may be more robust to radiation and material losses.

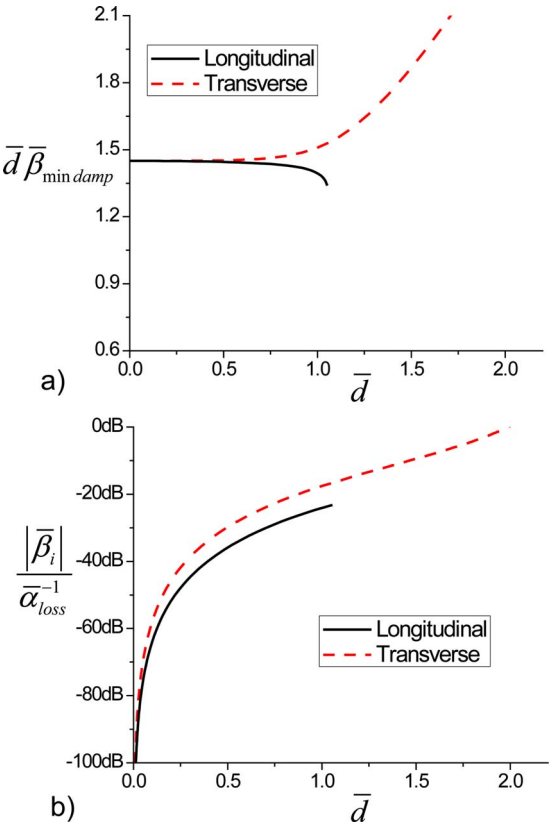

FIG. 7. (Color online) Value of $\bar{\beta}$ for achieving the minimum damping loss factor in the modal propagation in the (a) two polarizations and (b) corresponding damping factor.

In Fig. 7(b) we have reported the ratio between the minimum $|\bar{\beta}_i|$ and $\bar{\alpha}_{loss}^{-1}$ in a logarithmic scale, to show how the two modes may optimally behave in terms of losses. In this sense the longitudinal polarization offers a better performance, consistent with dipolar chains. These results represent final physical limitations for the guided propagation along quadrupolar chains, related to the same nature of these chains.

As we have done for dipolar chains, it is interesting to analyze how these expressions are simplified by applying NNA, i.e., for closely spaced nanoparticles. In this limit, Eq. (13) becomes

$$L{:}\,\bar{\beta}\bar{d} = \cos^{-1}[\mathrm{Re}[\bar{\alpha}_q^{-1}]/(240\bar{d}^{-5})],$$

$$T{:}\,\bar{\beta}\bar{d} = \cos^{-1}[-\mathrm{Re}[\bar{\alpha}_q^{-1}]/(60\bar{d}^{-5})], \tag{21}$$

and the amount of losses affect propagation as

$$L{:}\,\bar{\beta}_i = \bar{\alpha}_{loss}^{-1}\bar{d}^4/240,$$

$$T{:}\,\bar{\beta}_i = -\bar{\alpha}_{loss}^{-1}\bar{d}^4/60, \tag{22}$$

confirming that in the limit of small spacing the robustness to reasonable amount of losses is very strong (and it is four

times stronger in the longitudinal forward case than in the transverse backward case).

III. APPLICATION TO REALISTIC NANOPARTICLE GEOMETRIES

In order to consider the practical realization of these chains, realistic nanoparticle geometries need to be considered, taking into account frequency dispersion and realistic material losses. For simplicity let us consider the case of a chain of homogeneous spherical nanoparticles of radius a and permittivity ε. In the quasistatic limit, their quadrupolarizability may be written as

$$\mathrm{Re}[\bar{\alpha}_q^{-1}] = 15(k_0 a)^{-5}\frac{2\varepsilon + 3\varepsilon_0}{\varepsilon - \varepsilon_0}, \tag{23}$$

which goes into resonance as $\varepsilon=-3\varepsilon_0/2$.[14–18] Due to the geometrical requirement $d>2a$ and to the fact that $\frac{2\varepsilon+3\varepsilon_0}{\varepsilon-\varepsilon_0}>1$, for any $\varepsilon>\varepsilon_0$ a chain of dielectric particles cannot guide any laterally confined guided wave around the chain, since $(\bar{d}^5\,\mathrm{Re}[\bar{\alpha}_q^{-1}])>480$ for any $\varepsilon>\varepsilon_0$ (see Figs. 2 and 4). The region of guidance is concentrated near the quadrupolar resonance of plasmonic particles.

The regions of guidance (Figs. 3 and 5) may be written in closed form in terms of the nanosphere permittivity, as plotted in Fig. 8 for the two polarizations and for two different values of $\eta=d/a$. Notice that in the plots we vary $\bar{d}$ on the horizontal axis, keeping η fixed, implying that we also proportionally vary a.

The figures show some interesting features: first of all, even though the bandwidth of quadrupolar resonance for a plasmonic nanoparticle is vanishingly small when its size decreases,[13–16] closely spaced chains of small particles do not necessarily require to be close to the individual nanoparticle resonance since the range of guidance in terms of quadrupolarizability diverges as $\bar{d}^{-5}$ for small spacing. These two factors compensate, and therefore for tightly packed small nanoparticles the range of guidance for the permittivities remains interestingly a finite quantity in both polarizations, weakly sensitive to the permittivity of the material composing the particles. When the spacing is increased for fixed radius, the range of available permittivities narrows down, around the resonant value of $\varepsilon=-3\varepsilon_0/2$. The limiting values may be easily calculated in closed form as a function of the ratio η. For $\bar{d}\to 0$ we have

$$L{:}\,1-\frac{5\eta}{2\eta+15\xi(5)}<\frac{\varepsilon}{\varepsilon_0}<1-\frac{5\eta}{2[\eta-8\xi(5)]},$$

$$T{:}\,\frac{\varepsilon}{\varepsilon_0}\in\left[1-\frac{20\eta}{8\eta-15\xi(5)},1-\frac{5\eta}{2[\eta+2\xi(5)]}\right], \tag{24}$$

whereas when $\bar{d}\to\pi$ the only possible value for resonance remains,

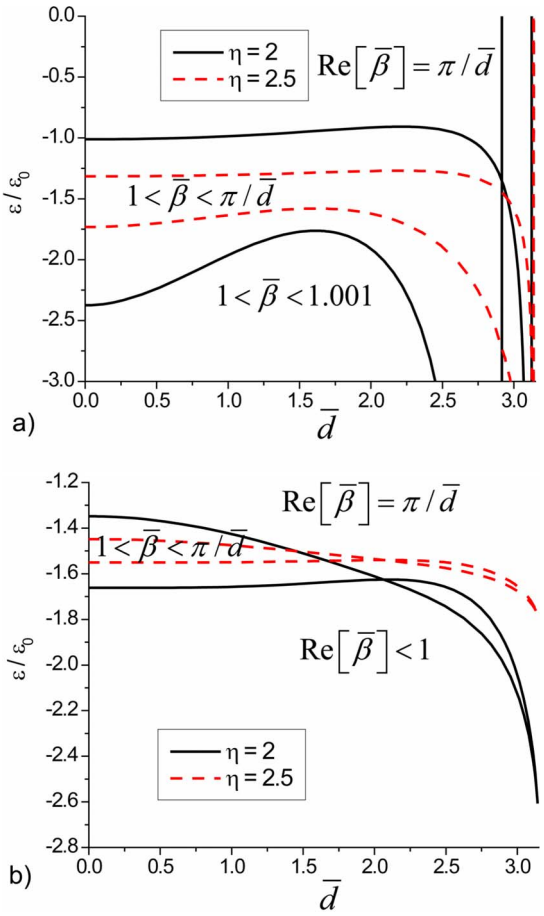

FIG. 8. (Color online) Range of guidance for the permittivity of homogeneous nanospheres vs their spacing for: (a) longitudinal polarization and (b) transverse polarization.

$$T{:}\,\frac{\varepsilon}{\varepsilon_0} = 1-\frac{5\eta}{2[\eta-\pi^2\xi(3)+2\xi(5)]}. \tag{25}$$

For increasing values of η all the quantities in Eqs. (24) and (25) tend to $\varepsilon=-3\varepsilon_0/2$, since for increasing spacing or decreasing size of the particles we expect to narrow down the bandwidth of the guided mode, concentrating the guidance around the frequencies for which $\mathrm{Re}[\bar{\alpha}_q^{-1}]\simeq 0$. Consistent with the dipolar case, longitudinal polarization offers better performance in terms of the range of permittivities that can support a mode.

Considering frequency dispersion, which is present in all plasmonic materials, the modal dispersion with permittivity may be directly translated into frequency dispersion for a given chain geometry. Consider, as an example, a chain of spherical nanoparticles with Drude-model permittivity, i.e., $\varepsilon(\omega)=\varepsilon_0(1-\frac{5\omega_0^2}{2\omega^2})$, surrounded by free space. Their individual quadrupolar resonance arises at frequency ω_0. In Fig. 9, we have reported the dispersion of guided β vs frequency for the two polarizations, in the case of $a=\lambda_0/20$ and $d=2.5a$. The two curves are delimited by the first Bragg resonance, for which with $\beta=\pi/d$ and by the light line for which $\beta=k_0$. The vertical axis is normalized to the wave number in free space at the central frequency ω_0. The slopes of the two

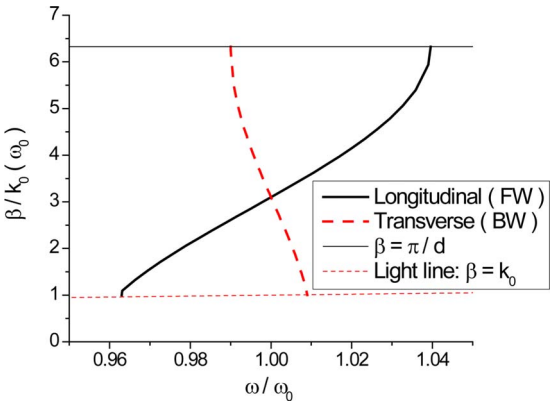

FIG. 9. (Color online) Frequency dispersion for a chain of spherical particles with radius $a=\lambda_0/20$ spacing $d=2.5a$ and permittivity following the Drude model $\varepsilon(\omega)=\varepsilon_0(1-2.5\omega_0^2/\omega^2)$.

curves clearly confirm the forward and backward nature of guided modes for longitudinal and transverse modes, respectively. Backward modes have consistently a smaller bandwidth (about 2% of the central frequency) compared to the forward mode (around 8%). These values of bandwidth are smaller than those achievable in the dipolar chains since the individual quadrupolar resonances have much narrower bandwidth of operation. However, these results are still impressive, considering that the fractional bandwidth of the isolated quadrupolar resonance for a nanoparticle may be written as

$$\mathrm{FBW} = \frac{30}{(k_0 a)^5} + \frac{(k_0 a)^5}{20}, \tag{26}$$

which for this size and permittivity is limited to about 10^{-4}. The achieved bandwidth, following the results in Fig. 8 may be further increased by decreasing d, i.e., packing the nanoparticles more closely together.

Introducing realistic Ohmic losses in the nanoparticles, we can employ Eq. (20) to optimize the damping factor. In the "quasistatic" limit, for a nanoparticle with complex permittivity $\varepsilon=\varepsilon_r+i\varepsilon_i$ we can write the following expression:

$$\bar{\alpha}_{loss}^{-1} = \frac{75\varepsilon_i (k_0 a)^{-5}}{(\varepsilon-\varepsilon_0)^2+\varepsilon_i^2}. \tag{27}$$

Similar to the dipolar chain, scaling down the size of a quadrupolar chain has two effects: on the one hand $\bar{\alpha}_{loss}^{-1}$ rapidly grows as $(k_0 a)^{-5}$, on the other hand its robustness to loss increases as $\bar{d}^{-4}$ [Eq. (22)]. Overall, the robustness of the quadrupolar chains to losses is quite impressive, decreasing linearly with η after a scaling, similar to the dipolar case. This is remarkable, considering the drastic sensitivity to losses that usually characterizes the individual quadrupolar resonance.[16]

Arrays of quadrupolar nanoparticles may be realized using metamaterial inclusions at lower frequencies, or optical nanoparticles in the IR and visible frequencies. In this sense, in Fig. 10 we have considered a chain of nanoparticles of radius $a=15$ nm and spacing $d=35$ nm excited with wavelength $\lambda_0=500$ nm. In the case of homogeneous nanospheres, the modal dispersion with permittivity is reported in Fig. 10(a) for longitudinal modes. A relatively wide range of permittivity would indeed support a longitudinal quadrupolar mode along this chain. For a permittivity below $\varepsilon=-1.87\varepsilon_0$ the chain would enter its leaky mode of operation, whereas for a permittivity above $\varepsilon=-1.2\varepsilon_0$ it would enter the cutoff region, with $\mathrm{Re}[\beta]=\pi/d$ and rapidly increasing $\mathrm{Im}[\bar{\beta}]$. It is interesting to note that the leaky mode operation, clearly seen in the left part of this plot, provides values of damping loss due to radiation much smaller than those in the dipolar chains or other similar classes of leaky-wave nanoantennas. This is consistent with Eq. (15) and the analogy with transmission-line propagation, which "better" guides energy along the chain and avoids localized radiation losses. The leaky beam arising from such nanoantennas, therefore, would be more directive than an analogous scenario at lower frequencies.

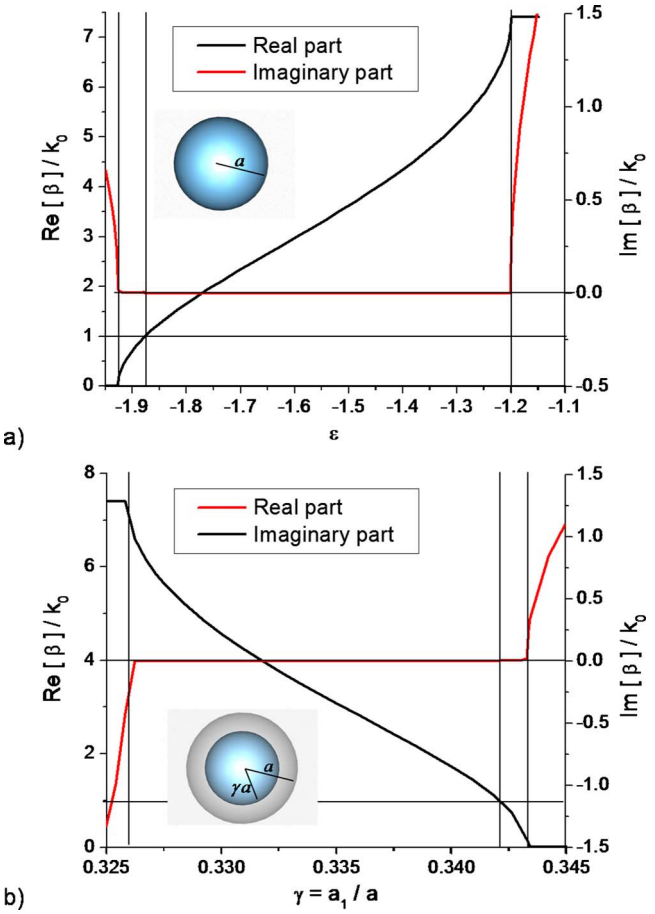

FIG. 10. (Color online) (a) Dispersion with the permittivity for a chain of homogeneous spherical particles with radius $a=15$ nm and spacing $d=2.25a$ at the wavelength $\lambda_0=500$ nm for longitudinally polarized modes; (b) dispersion for the same size, spacing, and polarization, but for a silicon carbide sphere covered with silver shell in terms of the ratio of radii $\gamma=a_1/a$.

If optical materials with these required values of permittivity are not readily available in nature, concentric nanoparticles may be employed for this purpose. Figure 10(b) shows the dispersion for nanoparticles made of a silver shell, which at $\lambda_0=500$ nm have a real part of permittivity $\mathrm{Re}[\varepsilon_{\mathrm{Ag}}]=$

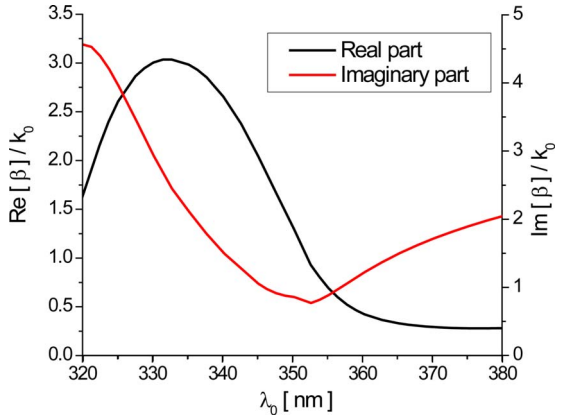

FIG. 11. (Color online) Frequency dispersion for the longitudinal modes supported by a chain of spherical silver particles with $a=20$ nm and $d=45$ nm.

$-9.77\varepsilon_0$, and a silicon carbide core ($\varepsilon_{SiC}=6.52\varepsilon_0$), keeping the same total radius a as in the previous geometry. In this case, we are able to tailor the resonance of the nanoparticles by changing the ratio of radii $\gamma=a_1/a$. This is shown, for the same wavelength of interest $\lambda_0=500$ nm in Fig. 10(b), providing similar results as in Fig. 10(a), but employing available optical materials and tailoring the response from leaky radiation through guidance up to Bragg reflection by simply changing γ.

Notice that in the previous example the spacing between neighboring particles is fairly large, leading to a relatively narrow "bandwidth" of parameters. This can be improved by making the nanoparticles more tightly coupled, as discussed above. As a final example, Fig. 11 shows the guided modes supported by a chain of spherical nanoparticles made of silver, considering also realistic data for material absorption,[32] using $a=20$ nm, $d=45$ nm as a function of the wavelength of operation λ_0. This somehow confirms the possibility of quadrupolar guidance even with simple homogeneous silver nanoparticle, working in the range around $\lambda_0=340$ nm.

IV. CONCLUSIONS

We have reported here a closed-form fully dynamic analysis of the guided modes supported by linear arrays of quadrupolar nanoparticles, extending our earlier work on dipolar chains. Following the heuristic analogy with oppositely flowing currents in paired wires in low-frequency transmission lines, we have shown how these quadrupolar lines provide guidance and robustness to radiation losses in their modal propagation. Despite the vanishing bandwidth of the quadrupolar resonance in each of the nanoparticles composing the chain, due to strong coupling among nanoparticles we have shown that the overall bandwidth of guidance is moderately large, even considering realistic losses and frequency dispersion of optical materials. We envision potential applications for optical nanotransmission lines and directive leaky-wave nanoantennas operating in the visible. It is worth underlining that the case of longitudinal dipolar chains over a perfect electric screen, analyzed in Ref. 33, and antisymmetric guided modes along parallel chains of nanoparticles, as analyzed in Ref. 34, would collapse to the solution for longitudinal modes derived here in the limit in which the spacing between chains or chain and screen tend to zero.

ACKNOWLEDGMENT

This work is supported in part by the U.S. Air Force Office of Scientific Research (AFOSR) Grant No. FA9550-08-1-0220.

*Author to whom correspondence should be addressed; alu@mail.utexas.edu

[1] M. Quinten, A. Leitner, J. R. Krenn, and F. R. Aussenegg, Opt. Lett. **23**, 1331 (1998).
[2] S. A. Tretyakov and A. J. Viitanen, Electr. Eng. **82**, 353 (2000).
[3] M. L. Brongersma, J. W. Hartman, and H. A. Atwater, Phys. Rev. B **62**, R16356 (2000).
[4] S. A. Maier, M. L. Brongersma, and H. A. Atwater, Appl. Phys. Lett. **78**, 16 (2001).
[5] S. A. Maier, P. G. Kik, H. A. Atwater, S. Meltzer, E. Harel, B. E. Koel, and A. A. G. Requicha, Nature Mater. **2**, 229 (2003).
[6] W. H. Weber and G. W. Ford, Phys. Rev. B **70**, 125429 (2004).
[7] A. F. Koenderink and A. Polman, Phys. Rev. B **74**, 033402 (2006).
[8] R. A. Shore and A. D. Yaghjian, Electron. Lett. **41**, 578 (2005).
[9] R. A. Shore and A. D. Yaghjian, IEICE Trans. Commun. **E88-B**, 2346 (2005).
[10] A. Alù and N. Engheta, Phys. Rev. B **74**, 205436 (2006).
[11] A. Alù and N. Engheta, Phys. Rev. B **75**, 024304 (2007).
[12] A. Alù, and N. Engheta, *Digest of IEEE Antennas and Propagation Society International Symposium* (IEEE, Honolulu, Hawaìi, USA, 2007), pp. 2897–2900.
[13] C. F. Bohren and D. R. Huffman, *Absorption and Scattering of Light by Small Particles* (Wiley, New York, 1983).
[14] A. Alù and N. Engheta, J. Appl. Phys. **97**, 094310 (2005).
[15] A. Alù and N. Engheta, J. Opt. Soc. Am. B **24**, A89 (2007).
[16] A. Alù and N. Engheta, IEEE Trans. Antennas Propag. **55**, 3027 (2007).
[17] M. Liu, T. W. Lee, S. K. Gray, P. Guyot-Sionnest, and M. Pelton, Phys. Rev. Lett. **102**, 107401 (2009).
[18] S. J. Oldenburg, G. D. Hale, J. B. Jackson, and N. J. Halas, Appl. Phys. Lett. **75**, 1063 (1999).
[19] N. Engheta, A. Salandrino, and A. Alù, Phys. Rev. Lett. **95**, 095504 (2005).
[20] N. Engheta, Science **317**, 1698 (2007).
[21] A. Alù and N. Engheta, J. Opt. Soc. Am. B **23**, 571 (2006).
[22] G. V. Eleftheriades and K. G. Balmain, *Negative Refraction Metamaterials: Fundamental Properties and Applications* (IEEE Press, Wiley, Hoboken, New Jersey, 2005).
[23] C. Caloz and T. Itoh, *Electromagnetic Metamaterials, Transmission Line Theory and Microwave Applications* (Wiley, IEEE Press, Hoboken, NJ, 2005).
[24] J. Van Bladel, *Electromagnetic Fields* (Taylor and Francis, New York, 1985).

[25] C. H. Papas, *Theory of Electromagnetic Wave Propagation* (Dover, New York, 1988).
[26] J. D. Jackson, *Classical Electrodynamics* (Wiley, New York, 1998).
[27] It should be noted that available definitions for the electric quadrupolarizability of a particle are various and different. Since the main effects of a quadrupolar moment are seen in nuclear fields (Ref. 26), where nonlinear effects are strong, often the quadrupolarizability relates the induced quadrupole moment to the square of the field through nonlinear effects. Here, however, we are interested in a linear regime of operation, for which the quadrupolarizability expresses the proportionality between induced quadrupole moment and symmetric part of the gradient of the electric field, as in Eq. (3).
[28] P. Morse and H. Feschbach, *Methods of Theoretical Physics* (Feschbach Publishing, Minneapolis, MN, 2005).
[29] J. A. Stratton, *Electromagnetic Theory* (Wiley-IEEE Press, New York, 2007).
[30] L. Lewin, *Polylogarithms and Associated Functions* (Elsevier North-Holland, New York, 1981).
[31] I. S. Gradshteyn and I. M. Ryzbik, *Table of Integrals, Series and Products*, 6th ed.(Academic Press, San Diego, CA, USA, 2000), pp. 44–45.
[32] P. B. Johnson and R. W. Christy, Phys. Rev. B **6**, 4370 (1972).
[33] A. J. Viitanen and S. A. Tretyakov, J. Opt. A, Pure Appl. Opt. **7**, S133 (2005).
[34] A. Alù, P. A. Belov, and N. Engheta (unpublished).